Numerical optimization for the geometrical configuration of ceramics perform in ZTAP/HCCI wear resistant composites based on actual particle model

Ruiju Xu (xuruiju2019@qq.com)
Kunming Institute of Physics
Tianlong Lu
Kunming University of Science and Technology
Jiankang Zhang
Sino-Precious Metals Holding Co.Ltd., Kunming,650106, China
Yehua Jiang
Kunming University of Science and Technology
Xiaoyu Chong
Kunming University of Science and Technology
Jing Feng
Kunming University of Science and Technology

Research Article

Keywords: Wear-resistant composites, Finite element analysis, Equivalent grain model, Thermal stress, Compressive stress

Posted Date: February 19th, 2021

DOI: https://doi.org/10.21203/rs.3.rs-206918/v1

Numerical optimization for the geometrical configuration of ceramics perform in HCCI/ZTA$_P$ wear resistant composites based on actual particle model

Ruiju Xu[1,2#], Tianlong Lu[1,#], Jiankang Zhang[3], Yehua Jiang[1], Xiaoyu Chong[1,*], Jing Feng[1]

[1]*Faculty of Materials Science and Engineering, Kunming University of Science and Technology, Kunming, 650093, China*

[2]*Kunming Institute of Physics, Kunming, 650223, China*

[3]*Sino-Precious Metals Holding Co., Ltd., Kunming, 650106, China*

Abstract

In order to reduce the thermal stress in high chromium cast iron (HCCI) matrix composites reinforced by zirconia toughened alumina (ZTA) ceramic particles, finite element simulation is performed to optimize the geometrical configuration of ceramics perform. The previous model simplifies the overall structure of the ceramic particle preform and adds boundary conditions to simulate the particles, which will cause uncontrollable error in the results. In this work, the equivalent grain models are used to describe the actual preform, making the simulation results closer to the actual experimental results. The solidification process of composite material is simulated and the infiltration between molten iron and ceramic particles was realized. Thermal stress in solidification process and compression stress distribution are obtained. The results show that adding 10mm round holes on the preform can improve the performance of the composite, which is helpful to prevent the cracks and increases the plasticity of the material.

Keywords: Wear-resistant composites; Finite element analysis; Equivalent grain model; Thermal stress; Compressive stress

[#]The authors contribute equally to this work

[*] Corresponding author, Email: chongxiaoyu007@163.com

1. Introduction

With the continuous advancement of the industrialization process, traditional single wear-resistant materials have gradually become difficult to meet the performance requirements of wear-resistant parts in the fields of metallurgy, electric power, and building materials [1, 2]. Ceramic particles reinforced composites such as high chromium cast iron (HCCI) matrix composites reinforced by zirconia toughened alumina (ZTA) ceramic particles (referred as HCCI/ZTA$_P$ composites hereinafter) composites is one of the most popular wear-resistant materials, which perfectly combines the high hardness of ZTA ceramic particles with the metal toughness of high-chromium cast iron, and makes full use of the complementary relationship between the two, giving excellent wear-resistance [3, 4].

HCCI/ZTA$_P$ composites still have some cracking tendency, which may affect the appearance and production stability [5-7]. The cracking of composite materials is related to plasticity and stress. Excellent plasticity and little thermal stress can reduce the possibility of cracking of composite materials [8]. If the thermal expansion coefficient between ceramic particles and metal is too large, the thermal stress in composites will increase accordingly. When the thermal stress is high, cracks may be initiated inside the composite material, especially at the interface between the ceramic particles and the metal. The continuous extension and propagation of cracks may eventually lead to the fracture of the composite material or even the entire layer peeling off [9, 10].HCCI/ZTA$_P$ composites materials also have the above problems. Therefore, in order to further improve the performance of HCCI/ZTA$_P$ composites, it is important to study and reduce their cracking tendency [11, 12].

In HCCI/ZTA$_P$ composites, the composite layer is designed as the working face and the rest is made of metal, which makes the composite to have high wear resistance and plasticity at the same time [13]. The HCCI/ZTA$_P$ composite is prepared by the infiltration method. When the molten metal penetrates into the aggregated particles, the temperature decreases, resulting in a poor combination of ceramic particles and metal. One of the great characteristics of composite materials is their designability [14]. According to actual demand, the ceramic particles are prepared into a preform with a

special structure and size, and then the preform is closely combined with the molten metal to prepare a ZTA_P/HCCI composite [15].

In order to reduce the thermal stress, we choose the ceramic particles preform of hexagon. In the hexagonal preform, the maximum distance the molten metal penetrates the preform is the same regardless of the direction. The hexagonal preform improves the uniformity of molten metal penetration and reduces the stress concentration [16, 17]. Although the hexagonal preform is used to reduce the tendency of the material to crack, the thermal stress in the material molding process still exists. In order to further improve the performance of the composite material, the structure of the preform needs to be optimized.

In the optimization of composite preform structure, the use of finite element method can reduce repeated experiments. In previous studies, due to the complexity of ceramic particle drawing and calculation, the ceramic particle preform is usually simplified as a whole. Thorough research found that the simplified model has some defects and cannot be used in a wider range. The establishment of equivalent particle model can further combine the model with the reality and reduce the error caused by the model [18].

The finite element analysis software COMSOL Multiphysics® method is used to model the stress fields in the solidification process and compression process of the HCCI/ZTA_P composite material [19]. COMSOL Multiphysics® is a large-scale advanced numerical simulation software [20, 21]. The version of COMSOL Multiphysics® used in this paper is 4.5a. This study systematically analyzes the influence of the geometric model in the finite element software on the calculation results, which benefits the design and development of porous perform.

2. Modeling and experiments

2.1 Theory and equations

In the process of solidification, the temperature of each position of mold and liquid metal is different and liquid metal solidifies rapidly, so it is in the process of unsteady heat transfer, and the heat transfer equation can be written[22]:

$$\rho C_P \frac{\partial T}{\partial x} = \frac{\partial}{\partial x}\left(\lambda \frac{\partial T}{\partial x}\right) + \frac{\partial}{\partial y}\left(\lambda \frac{\partial T}{\partial y}\right) + \frac{\partial}{\partial z}\left(\lambda \frac{\partial T}{\partial z}\right) + \rho Q \quad (1)$$

In the equation;ρ is density; C_P is Heat Capacities; λ is thermal conductivity; T is transient-temperature; Q is heat; the coordinates x, y, and z are called the relative coordinates of subsystem.

Since the temperature of each point is very different in the solidification process, there is a variable internal stress in the casting. If the casting is can be regard as linear elasticity body, when the internal stress is less than the yield limit, with the process of elastic deformation, we can use Hooke's law equation to describe it.

$$\begin{cases} \varepsilon_{xx} = \frac{1}{E}\left[\sigma_{xx} - v\left(\sigma_{yy} + \sigma_{zz}\right)\right] \\ \varepsilon_{yy} = \frac{1}{E}\left[\sigma_{yy} - v(\sigma_{xx} + \sigma_{zz})\right] \\ \varepsilon_{zz} = \frac{1}{E}\left[\sigma_{zz} - v\left(\sigma_{xx} + \sigma_{yy}\right)\right] \rightarrow \varepsilon_{ij} = \frac{1+v}{E}\sigma_{ij} - \frac{v}{E}\delta_{ij}\sigma \\ \varepsilon_{xy} = \frac{1}{2G}\sigma_x \\ \varepsilon_{yz} = \frac{1}{2G}\sigma_{yz} \\ \varepsilon_{zx} = \frac{1}{2G}\sigma_{zx} \end{cases} \quad (2)$$

Where E is Young's modulus; $\sigma = \sigma_{ii+\sigma_{11}} + \sigma_{22+}\sigma_{33}$; v is Poisson's ratio; Unit tensor$\varepsilon_{ij} = \frac{1}{2}\gamma_{ij}$; shear modulus $G = \frac{E}{2(1+v)}$.

Then the internal stress is larger than the yield limit, the casting has more deformation. Total strain is composed of elastic strain and plastic strain, $\sigma_{ij}=\sigma^e{}_{ij}+\sigma^p{}_{ij}$. This equation can be treated as elastic plastic linear hardening model. Elastic deformation and plastic deformation are linear, and the constitutive equation can be written as[23]:

$$\sigma = \begin{cases} E\varepsilon & \varepsilon \le \varepsilon_s \\ \sigma_s + E_1(\varepsilon - \varepsilon) & \varepsilon > \varepsilon_s \end{cases} \quad (3)$$

In this equation, σ is strain; E is Young's modulus; ε is stress; ε_s is yield strength;

2.2 The establishment and optimization of geometric model

The service life of high chromium cast iron workpieces is shorter. Composite materials have many advantages over single materials. In the manufacturing process of HCCI/ZTA$_P$ composites, the ZTA ceramic particles are prepared in advance into a porous preform. The preform makes the ZTA ceramic particles and the high chromium cast iron more tightly combined, and the ceramic particles are not easy to fall off when

subjected to impact. In order to further improve the performance of the HCCI/ZTA$_P$ composites, it is necessary to optimize the structure of the preforms.

During the casting process, the molten metal can fill the circular holes and increase the proportion of metal. In the application process of HCCI/ZTA$_P$ composite material, it is found that the particle aggregation position is more prone to crack, so the circular hole is added in this position. In order to reduce repeated experiments and save costs, the finite element software COMSOL Multiphysics was used to simulate HCCI/ZTA$_P$ composite materials. The simulation results included thermal stress, temperature field, phase transition field during solidification and stress strain of the casting under load.

The shape of ZTA ceramic particles is arbitrary polygon, and there are many particles in each preform. If all the particles are drawn, the workload is large. In previous simulations of ceramic metal matrix composites, most of the preforms of ceramic particles were considered as a whole. As shown in Figure 1, a simplified model is established to analyze the effect of adding circular holes, and the simulation results are far from the experimental results. The simplified model is optimized, and the equivalent particle grain model is established, as shown in figure 2. In the optimization model, the calculated results are in good agreement with the experimental results.

In the establishment of the geometric model of the finite element software, in order to reduce the calculation time and reduce the modeling workload, the simplified geometric model is often used. As shown in figure 2, there are gaps between the particles because when the three-dimensional hexagonal porous prefabrication is simplified to a two-dimensional model, only one layer of particles is selected to project the two-dimensional model. In this way, the stacking of particles in the three-dimensional space can effectively avoid the influence on the two-dimensional geometric model. Reasonably simplify the model and improve the calculation efficiency.

After the simulation is completed, the calculation results are verified by experiments. Make reasonable and effective adjustments to the established finite element model so that the established finite element model can be used in a wider range.

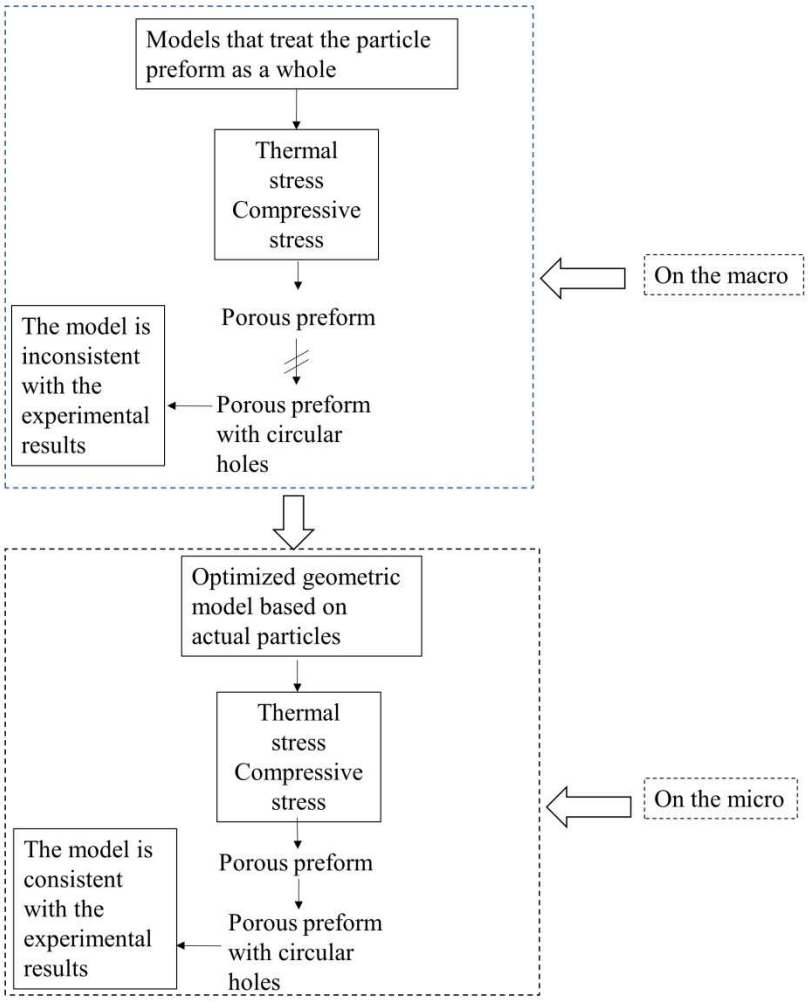

Figure.1. The flowchart of geometric model optimization for HCCI/ZTA$_P$ materials

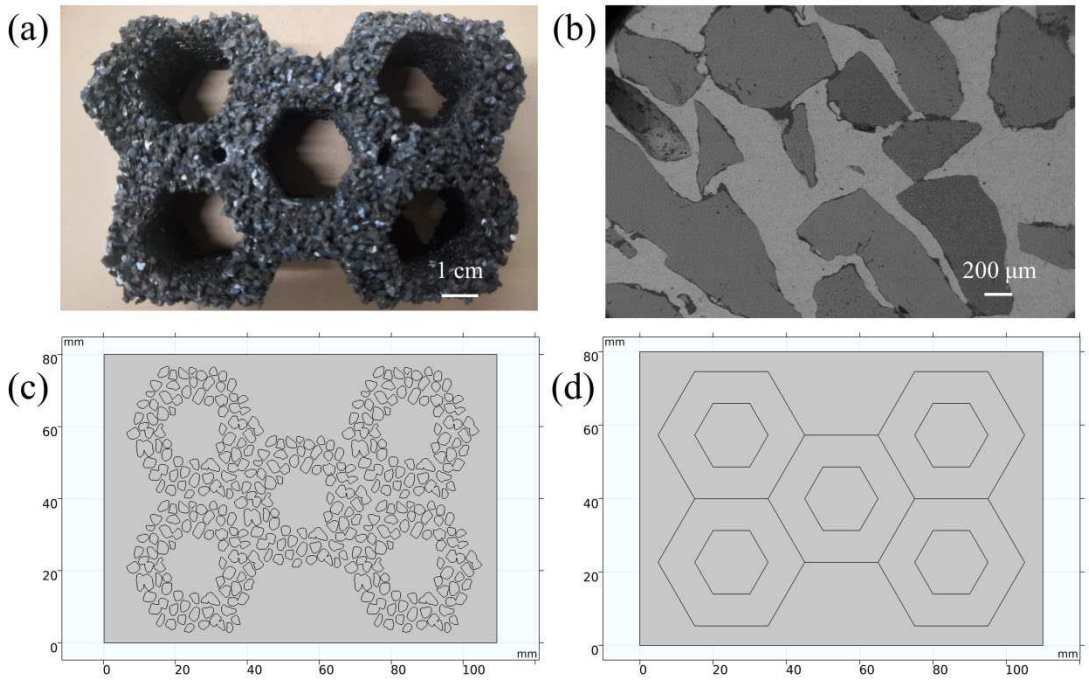

Figure.2. ZTA ceramic particles and geometric model of HCCI/ZTA$_P$ composites. (a)Porous perform, (b)The composite zone of HCCI/ZTA$_P$ composites, (c)Optimized geometric model based on actual particles(d)Initial geometric model.

The material parameters have great influence on the result of finite element calculation. The material parameters required for the simulation calculation in this paper are obtained by experiments and literature. The material parameters of ZTA ceramic particles and HCCI are shown in table 1.

Table 1. Material parameters.

	E/ GPa		(μ)		α(10^{-5}/°C^{-1})	
Temperature/°C	ZTA	HCCI	ZTA	HCCI	ZTA	HCCI
25	3.00	205	0.245	0.291	0	0
700	2.95	140	0.248	0.316	0.9	1.386
1300	2.82	0	0.252	0.500	0.91	2.370
1570	2.75	0	0.258	0.500	0.92	2.675

Note: *E*—plastic modulus, μ—Poisson's ratio, α—coefficient of thermal expansion

2.3 Experiments

In order to test the plasticity and wear resistance of the HCCI/ZTA$_P$ composite material, a systematic test was carried out on the composite material to further

determine the influence of the preform structure. The test mainly consists of two parts. SHT4305 universal testing machine was used to measure the compression properties of HCCI/ZTA$_P$ composites. The size of the compression test sample is 10×10×25mm, the tonnage of the universal testing machine is 30 tons, and the compression speed during the test is 0.5mm/min.

The wear performance test of HCCI/ZTA$_P$ composite is necessary. Excellent abrasion resistance is the most important criterion for testing the performance of wear-resistant composite materials. HCCI/ZTA$_P$ composites is mainly used in the mineral processing, cement manufacturing, and paper manufacturing industries, and most of the working conditions are three-body abrasive wear. In order to simulate the use performance of HCCI/ZTA$_P$ composites under actual working conditions as much as possible, tested the HCCI/ZTA$_P$ composites using mmh-5 three-body abrasive wear tester. The track material of the tester is M2 tool steel, hardness 820 ~ 860Hv, outer diameter 380mm, width 20mm.The type and size of abrasives are selected according to different working conditions. In this paper, quartz sand is used for abrasives, the hardness is 1000~1200Hv, the test load is 40N, and the rotating speed is 30r/min.

The nano-indenter was used to test the Young's modulus of the HCCI/ZTA$_P$ composites, and were characterized on the metal matrix around the positions of the sharp corners and rounded corners of the particles, Test the Young's modulus of HCCI/ZTA$_P$ composites with nano-indenter, and collect 100 points of indentation data on each modulus map.

The wear resistance of materials can be measured with mass reduction, volume reduction, and so on. The volume loss measured by a measuring cylinder with small changes can easily cause errors in human readings. Therefore, under the same wear conditions, the mass loss Δm is used to evaluate the wear performance of the material. The formula for calculating material loss is as follows:

$$\Delta m = m_1 - m_2 \quad (4)$$

m_1 and m_2 respectively represent the mass of samples before and after wear.

3. Results and discussion

3.1 Simulation based on simplified entire model

In the simulation of thermal stress in the solidification process of HCCI/ZTA$_P$ composite materials in this paper, the thermal stress distribution at 10s is selected for all the simulation results, because the thermal stress changes significantly before and after 10s. Compared with the scale at the right of the figure, red indicates greater stress and blue indicates less stress. In figure 3(a), stress concentration appeared on the edge of the preform, especially in the middle position, the upper side and the lower side of the preform appeared red. Comparing to the right scale of figure 3(a), it shows that the stress is enormous here. Blue appears at the place where the particles gather, that is, the intersection of the hexagonal hole walls, indicating that the stress is small here. In the geometric model in figure 3(c), circular holes are added to the particle aggregates of the preform. The stress distribution in figure 3(c) is similar to figure 3(a), except that there is a more obvious stress concentration around the circular holes. The stress distribution around the circular hole of the perform in figure 4 is similar to that in figure 3

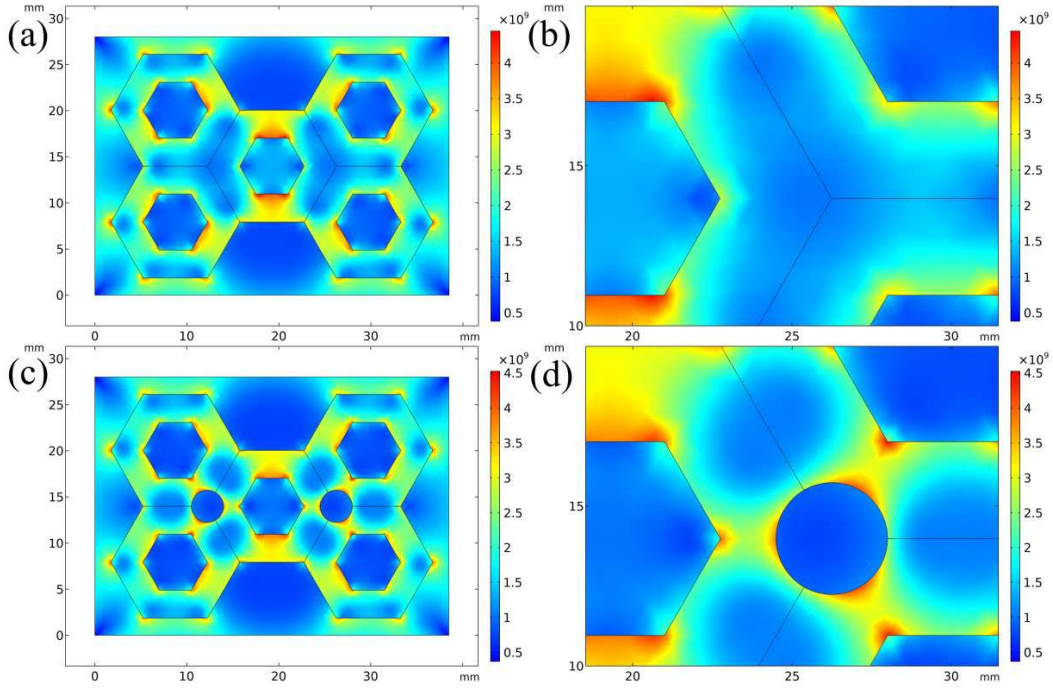

Figure3.Thermal stress distribution during solidification in the simplified model. (a)Initial perform, (b)Partial enlarged view of the initial perform, (b)Preform with circular holes added, (d) Partial enlarged view of the perform with circular holes added.

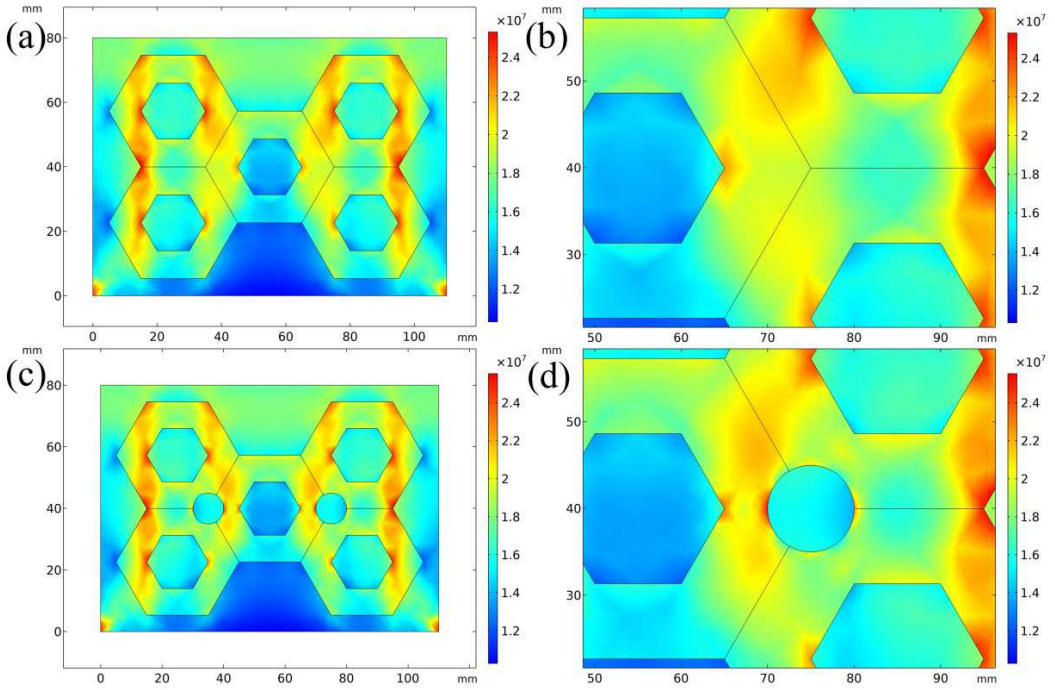

Figure 4.Compressive stress in the simplified model. (a)Initial perform, (b)Partial enlarged view of the initial perform, (b)Preform with circular holes added, (d) Partial enlarged view of the perform with circular holes added.

In order to make the final calculation results more intuitive, the results were post-processed and a stress transversal comparison chart was drawn. First draw a 2D transversal in the geometric model, because the main observation part is around the circular hole, that is, where the particles gather, so the 2D transversal passes through the circular hole. The ordinate of the stress graph is the stress value on the section line, and the abscissa is the X axis coordinate of the model, as shown in figure 5. In the simplified model, the circular hole coordinates are (12,14), (27,14). Figure 5(c) is a line graph of solidification stress. In figure 5(c), the preform with circular holes has a significant increase in the stress at the abscissas 12 and 27, compared with the preform without circular holes. Figure 5(d) is a comparison chart of compressive stress. The general trend of the curve is the same as that of figure 5(c), and the location stress of the circular hole will increase significantly.

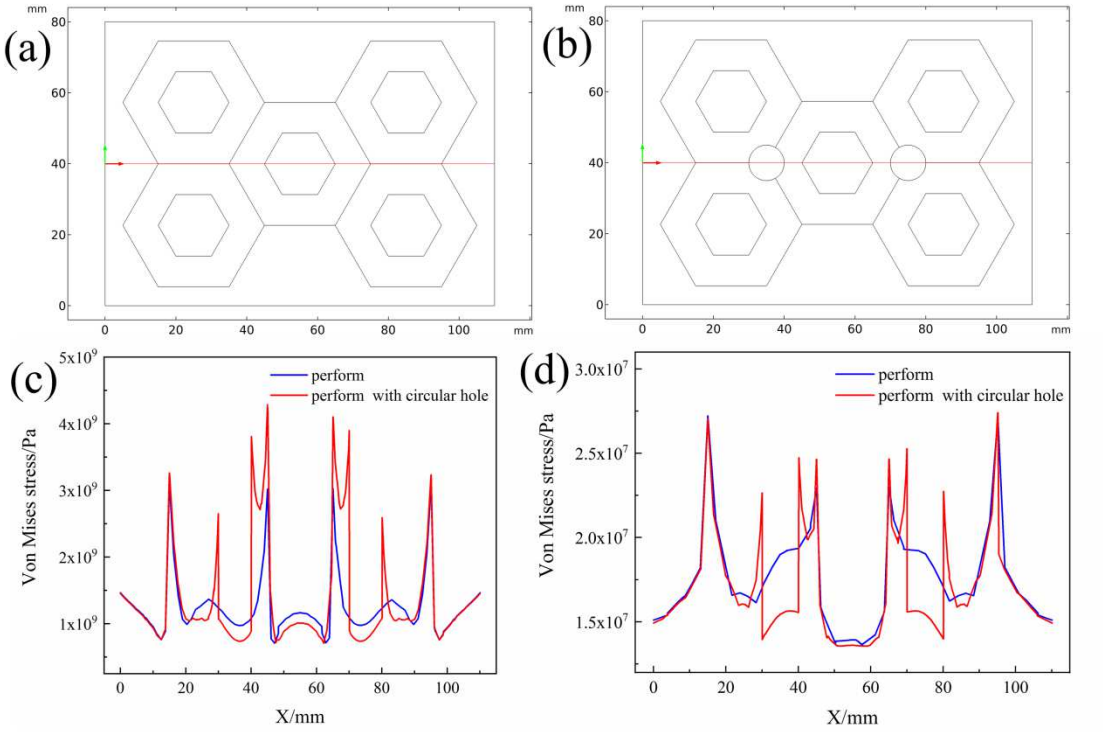

Figure 5.The position of the 2D transversal of the simplified model and stress transversal comparison, (a)Initial perform, (b)Partial enlarged view of the initial perform, (b)Preform with circular holes added, (d) Partial enlarged view of the perform with circular holes added.

In order to make the final calculation results more intuitive, the results were post-processed and a stress transversal comparison chart was drawn. First draw a 2D transversal in the geometric model, because the main observation part is around the circular hole, that is, where the particles gather, so the 2D transversal passes through the circular hole. The ordinate of the stress graph is the stress value on the section line, and the abscissa is the X axis coordinate of the model, as shown in Figure 5. In the simplified model, the circular hole coordinates are (12,14), (27,14). Figure 5(c) is a line graph of solidification stress. In figure 5(c), the preform with circular holes has a significant increase in the stress at the abscissas 12 and 27, compared with the preform without circular holes. Figure 5(d) is a comparison chart of compressive stress. The general trend of the curve is the same as that of figure 5(c), and the location stress of the circular hole will increase significantly.

3.2 Simulation based on equivalent grain model

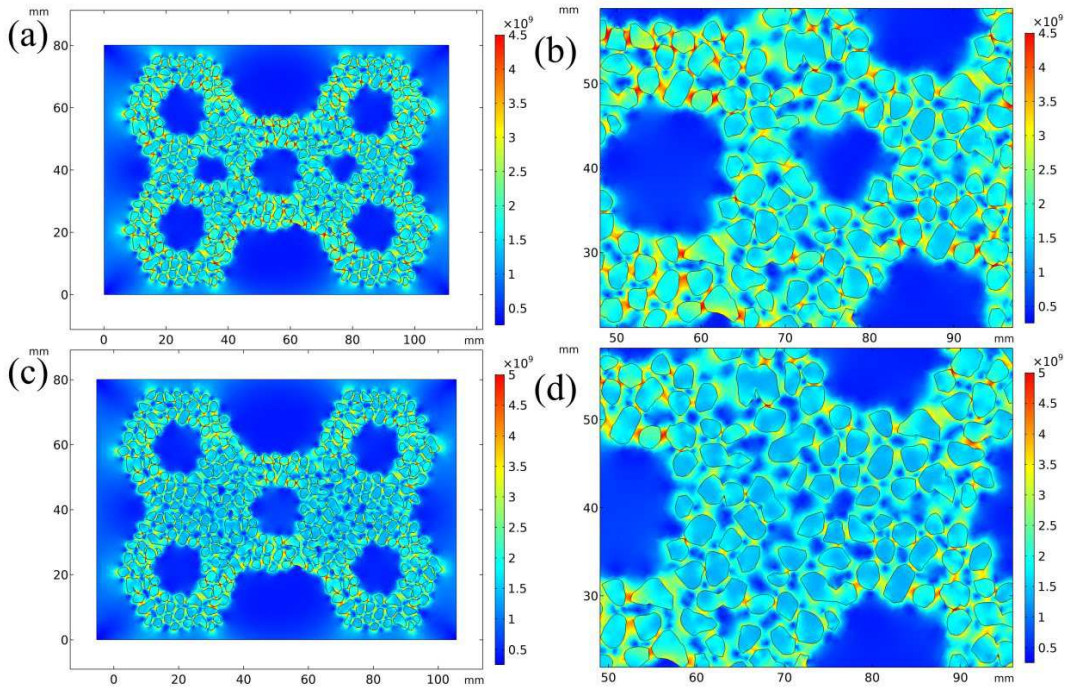

Figure 6.Thermal stress distribution during solidification in the optimized model. (a)Initial perform, (b)Partial enlarged view of the initial perform, (c)Preform with circular holes added, (d) Partial enlarged view of the perform with circular holes added.

Figure 6 shows the thermal stress distribution of HCCI/ZTA$_P$ composite material model based on actual particles, which is similar to figure 3. However, in Figure6, the ZTA ceramic particles are no longer simplified as a whole preform, but established as individual particles, it can be observed that most of the particles around appear red. The shape of ZTA ceramic particles is not uniform, and the stress is higher than the surrounding value, especially at the sharp point of the particles. The thermal stress distributions in figure6 (b) and figure 3(b) are obviously different. The circular hole of the preform in figure6 (b) appears blue, indicating that the stress is small here, and figure 3(b) The calculation results of stress concentration around the circular hole are opposite. The degree of simplification and drawing methods of geometric models leads to different calculation results.

The geometric model used to simulate the compressive stress in figure7 is the same as figure6. In figure 7, comparing with the scale on the right, the stress is concentrated

on the upper part of the model and the preform, especially the edges on both sides of the ceramic preform, which are yellow-green.the aggregate of the preform particles in figure7 (a) is green, indicating that the stress is small here. In figure7 (b), circular holes are added at the aggregates of the preform. The positions of the circular holes are green and yellow, indicating that there is no obvious stress concentration.

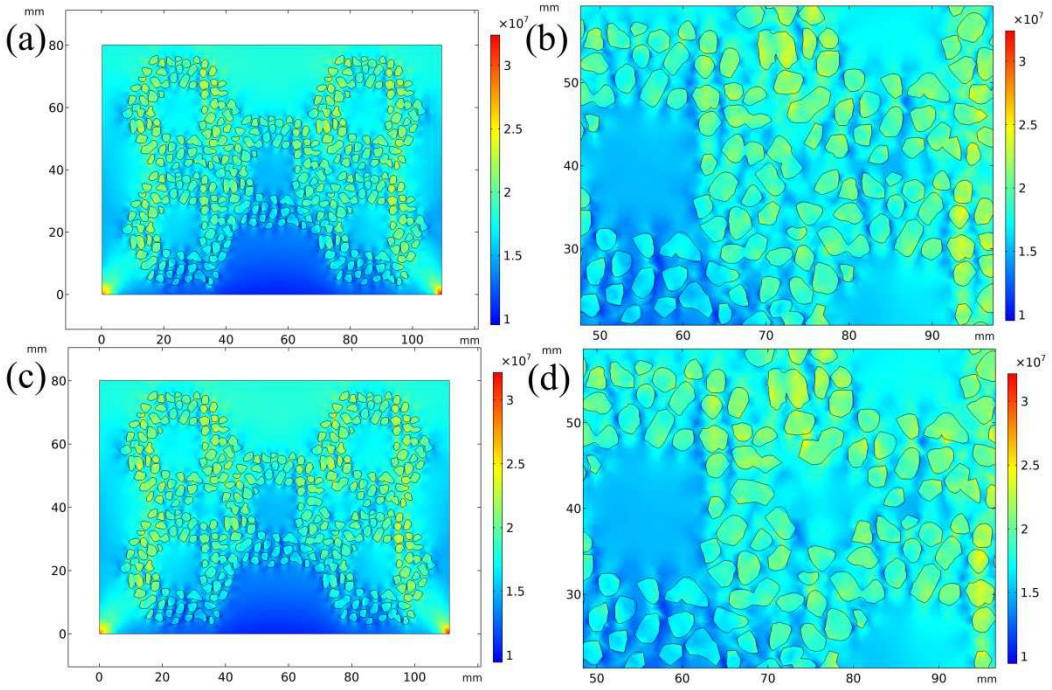

Figure 7. Compressive stress in the optimized model. (a) initial perform, (b)Partial enlarged view of the optimized perform, (c)Preform with circular holes added, (d) Partial enlarged view of the perform with circular holes added.

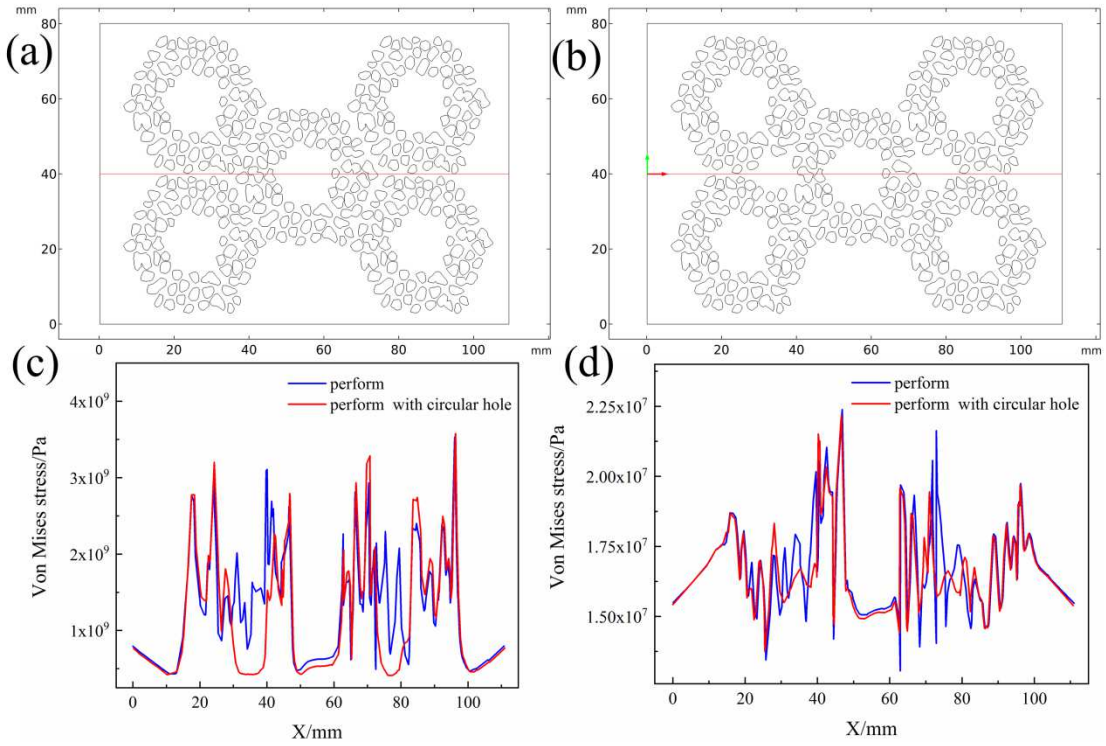

Figure.8.The position of the 2D transversal of the optimized model and stress transversal comparison. (a) Initial perform, (b) Preform with circular holes added, (c)Solidification stress, (d) compression stress.

In the model based on actual particles, the circular hole coordinates are (12, 14) (27, 14). Figure 8 is a comparison diagram of solidification stress, comparing the effect of the presence or absence of circular holes on stress. The stress of the preform with circular holes showed a significant reduction at the abscissas 12 and 27, and its position basically coincided with the position of the circular holes. The stress of the remaining coordinates of the preform with circular holes has a small increase. In Figure 8(a) and figure 8(b), the two curves are basically coincident, except in the prefabricated body with round holes, the stress near the round hole coordinates drops significantly.

3.4 Experimental validations

It can be seen from figure 9 that in the wear test, the mass loss of the composite material using the optimized preform and the composite material without the original preform is not much different, indicating that the wear resistance is not significantly sacrificed can also improve the overall plasticity of the HCCI/ZTA$_P$ composites.

The porous preform was optimized by adding small cylindrical holes at the particle aggregation point, which changed the volume fraction of ceramic particles in the

HCCI/ZTAP composites. The content of ZTA ceramic particles in the composite material was an important factor affecting its mechanical properties. As shown in figure. 9, the compression strength and compression deformation of sample which has preforms with circular holes added increase significantly compared with that of sample which has initial preform, indicating that small circular holes at the concentration of ZTA ceramic particles are conducive to improving the strength and plasticity of the HCCI/ZTAP composites. The addition of small cylindrical holes at the agglomeration of porous preform particles will increase the content of the metal matrix, thus increasing the compressive strain of the HCCI/ZTAP composites under compressive stress and also affecting its compressive strength. When the stress reaches the peak value, it can be considered that the damage has already occurred in the specimen. With the continuous increase of strain, the internal damage of the material is also accumulating, the strain resistance gradually decreases, and finally the shear failure occurs

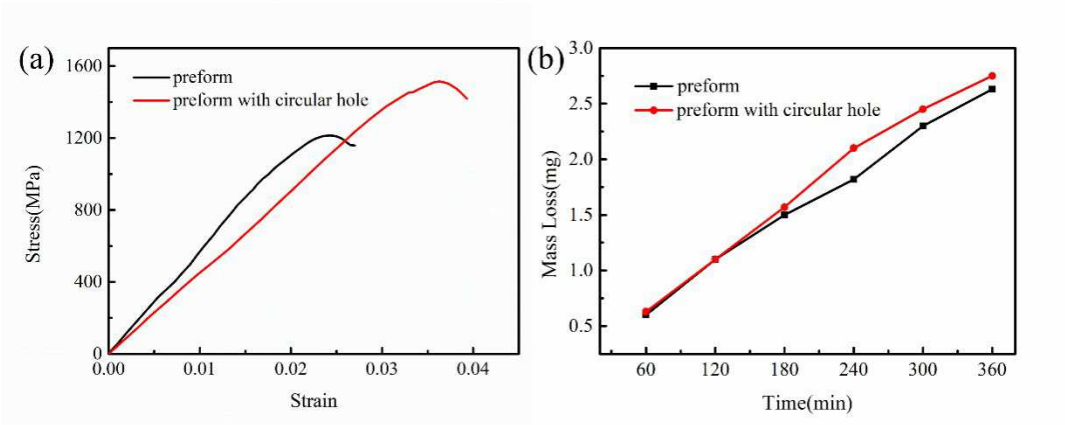

Figure 9.Compression stress-strain curve of HCCI/ZTAP composite material and mass loss of three-body abrasive at the junction of composite honeycomb walls

The micro-analyses of hardness of all samples are shown in Fig. 10.Figure 10 (c) and figure 10 (d) are compared with the enlarged partial view of particle stress. In the simulation, stress concentration tends to occur around sharp corners. In the test, the modulus near the sharp corner particles is greater than the modulus of the metal matrix near the round corners, which further verifies the rationality of the model which based on the actual particle.

A circular hole was added to the particle aggregation of the ZTA ceramic particle

preforms, which had three functions. The first is to reduce the volume fraction of ceramic particles in the HCCI/ZTAP composite material and reduce the residual stress; the second is to reduce the agglomeration of the ceramic particles of the preform; the third is to increase the volume fraction of the metal matrix with better plasticity to a certain extent to hinder crack propagation. The plasticity of HCCI/ZTAP composite materials decreases with the increase of residual stress. The residual stress is affected by the volume fraction of. The volume fraction of ceramic particles decreases and the residual stress becomes relatively small. The addition of circular holes in the ZTA ceramic particle preform can reduce cracks because the crack instability tends to extend along a straight line. When cracks are generated in the composite zone of HCCI/ZTAP composite material, the cracks are easily extended along the hexagonal hole wall in the precast to generate crack propagation. The circular hole increases the content of high chromium cast iron matrix at the junction of hexagonal hole wall, hinders the crack propagation, and thus plays a role in toughening the structure.

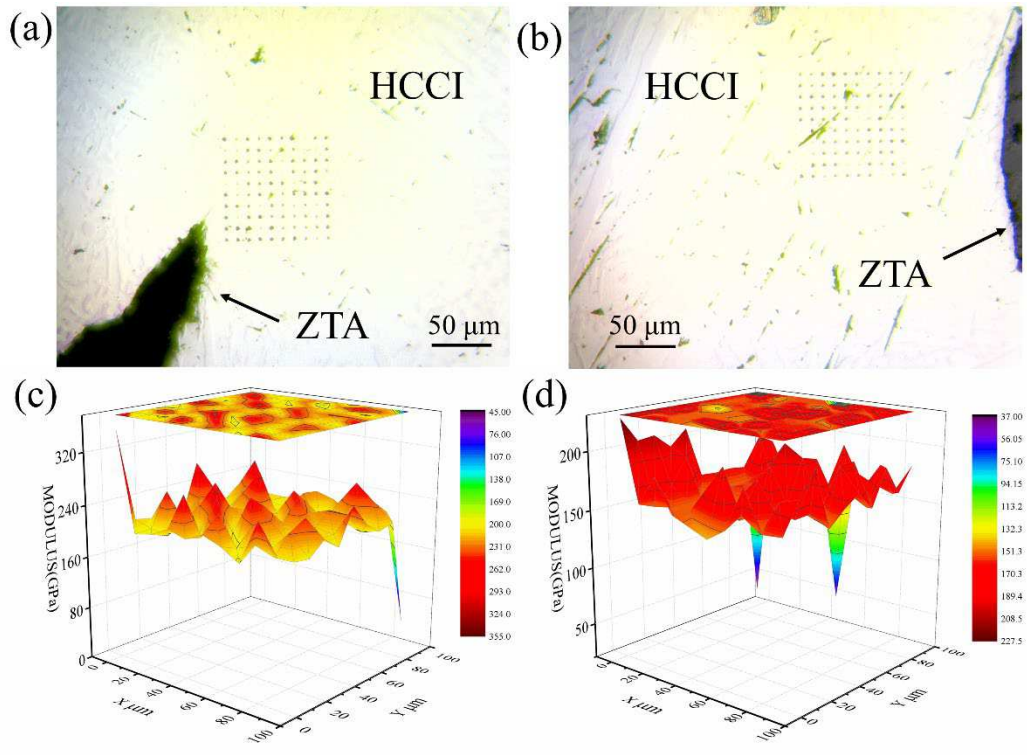

Figure 10.Indentation distribution of composite materials and the distribution of Young's modulus around the particles of composite materials.(a)The shape of the particles is sharp,(b)The shape of the particles is rounded,(c)The shape of the particles is sharp,(d)The shape of the particles is rounded.

4. Conclusion

The large difference in thermal expansion coefficient between high chromium cast iron and ceramic particles causes cracks in the composite material. The solidification and compression process of HCCI/ZTA$_P$ composite materials are simulated by using the finite element software COMSOL Multiphysics, and the numerical values and distributions of stresses analyzed based on simplified entire model and equivalent grain model for preform. According to the calculation results, the prefabricated structure is optimized. By analyzing the simulation and experimental results, it can be concluded that the addition of circular holes to the hexagonal porous preform will lead to a decrease in thermal stress and compressive stress during solidification.

The experimental results show that adding circular holes has little effect on the wear performance of HCCI/ZTA$_P$ composites, and can improve the plasticity of the composites. After the optimization and adjustment of the model, the simulation results tend to be consistent with the experimental results. It shows that the established model is not suitable for all experimental conditions, and the model needs to be adjusted in time according to the experimental conditions and purposes. The methods discussed in this paper may provide important reference value for the simulation and optimization of processing parameters in various metal matrix composite casting systems.

Acknowledgments

This work was supported by the Rare and Precious Metals Material Genetic Engineering Project of Yunnan Province (202002AB080001-1) and the Scientific Research Fund of Education Department of Yunnan Province (No. 2019J0031)

Reference

1. Jha, P.; Gupta, P.; Kumar, D.; Parkash. Journal of Composite Materials 2014**,** 48, (17), 2107-2115.
2. Ru, J.; Jia, Y.; Jiang, Y.; Feng, J.; Zhou, R.; Hua, Y.; Wang, D. Surface Engineering 2017, 353-361.
3. Du, J.; Chong, X. Y.; Jiang, Y. H.; Feng, J. International Journal of Heat Mass Transfer 2015**,** 89, 872-883.
4. Miserez, A.; Mortensen, A. Acta materialia 2004**,** 52, (18), 5331-5345.
5. Shuowei, Y.; Zichun, Y. Computational Materials Science 2017**,** 131, 202-208.
6. Chong, X.; Wang, G.; DU, J.; Jiang, Y.; Feng, J. Acta Metall Sin 2017**,** 54, (2), 314-324.
7. Liu, Z.; Xu, R.; Tan, P.; He, H.; Jiang, Y.; Sui, Y. Materials Resarch Express 2020**,** 6, (12), 1265d9.
8. Wang, J.; Cheng, Q.; Tang, Z. Chemical Society Reviews 2012**,** 41, (3), 1111-1129.
9. Xu, R.; Chong, X.; Zhou, Y.; Jiang, Y.; Feng, J. Materials Research Express 2019**,** 6, (10), 106551.
10. Takenaka; Koshi. Science technology of advanced materials 2012.
11. Jiang, L.; Ling, J.; Jiang, L.; Tang, Y.; Li, Y.; Zhou, W.; Gao, J. Energy conversion management 2014**,** 81, 10-18.
12. Zhou, Y.; Liu, Q.; Hu, M.; Xu, G.; Xu, R.; Chong, X.; Feng, J. International Journal of Quantum Chemistry 2020**,** 120, (10), e26219.
13. Wei, X.; Xiong, J.; Wang, J.; Xu, W. Science China Technological Sciences 2020, 1-23.
14. Wang, J.; Nartey, M. A.; Luo, Y.; Wang, H.; Scarpa, F.; Peng, H.-X. Composite Structures 2020**,** 233, 111580.
15. Guo, X.; Song, K.; Liang, S.; Wang, X.; Zhang, Y. Tribology Transactions 2014**,** 57, (2), 283-291.
16. Dong, C.; Zhou, J.; Yin, Y.; Guo, Z. Ceramics–Silikáty 2016**,** 60, (2), 129-135.
17. Liu, Y.; Zhou, J.; Shen, T. Materials Design 2013**,** 45, 67-71.
18. Waghray, A.; Donaldson, R.; La Forest, M. L., Composite materials including ceramic particles and methods of forming the same. Google Patents: 2016.
19. Salvi, D.; Boldor, D.; Aita, G.; Sabliov, C. Journal of food engineering 2011**,** 104, (3), 422-429.
20. Leckey, C.; Rogge, M.; Parker, F. In Microcracking in composite laminates: Simulation of crack-induced ultrasound attenuation, AIP Conference Proceedings, 2013; American Institute of Physics: pp 947-954.
21. Li, J.; Yang, Q.; Niu, P.; Jin, L.; Meng, B.; Li, Y.; Xiao, Z.; Zhang, X. Physics Procedia 2011**,** 22, 150-156.
22. Fiveland, W. Journal of Thermophysics Heat Transfer 1988**,** 2, (4), 309-316.
23. Chen, G.; Chen, L.; Zhao, G.; Zhang, C.; Cui, W. Journal of Alloys Compounds 2017**,** 710, 80-91.

Figures

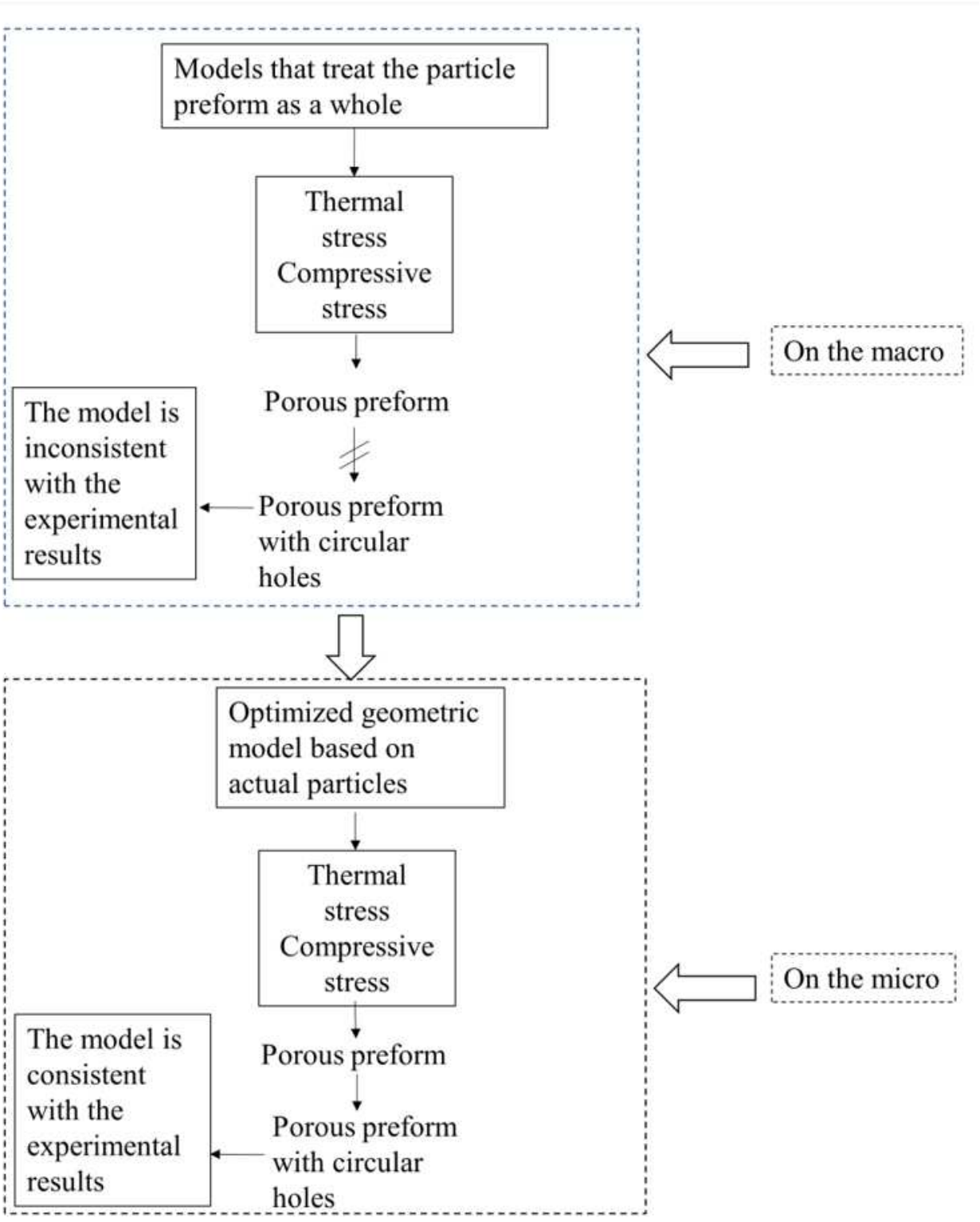

Figure 1

The flowchart of geometric model optimization for HCCI/ZTAP materials

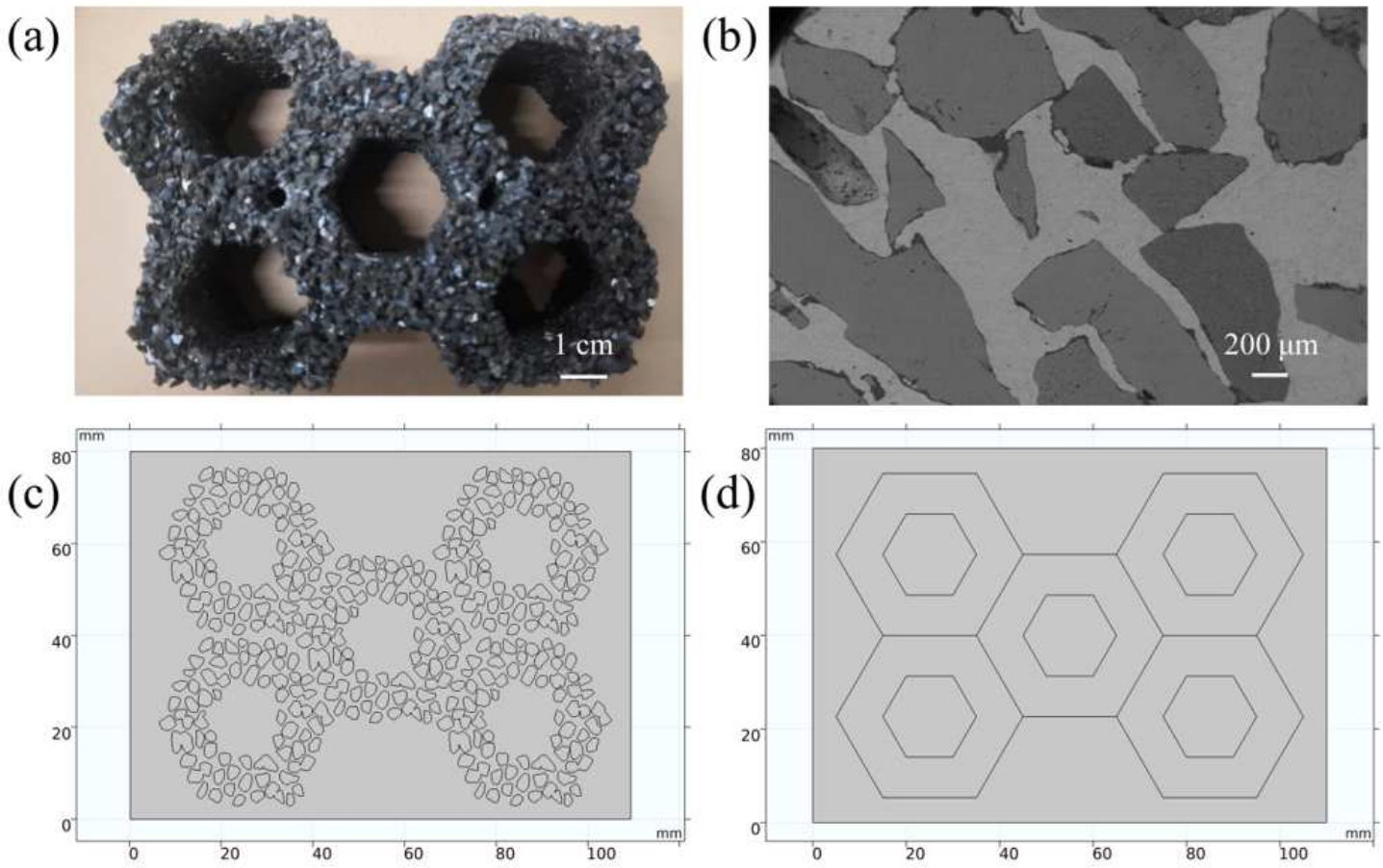

Figure 2

ZTA ceramic particles and geometric model of HCCI/ZTAP composites. (a)Porous perform, (b)The composite zone of HCCI/ZTAP composites, (c)Optimized geometric model based on actual particles(d)Initial geometric model.

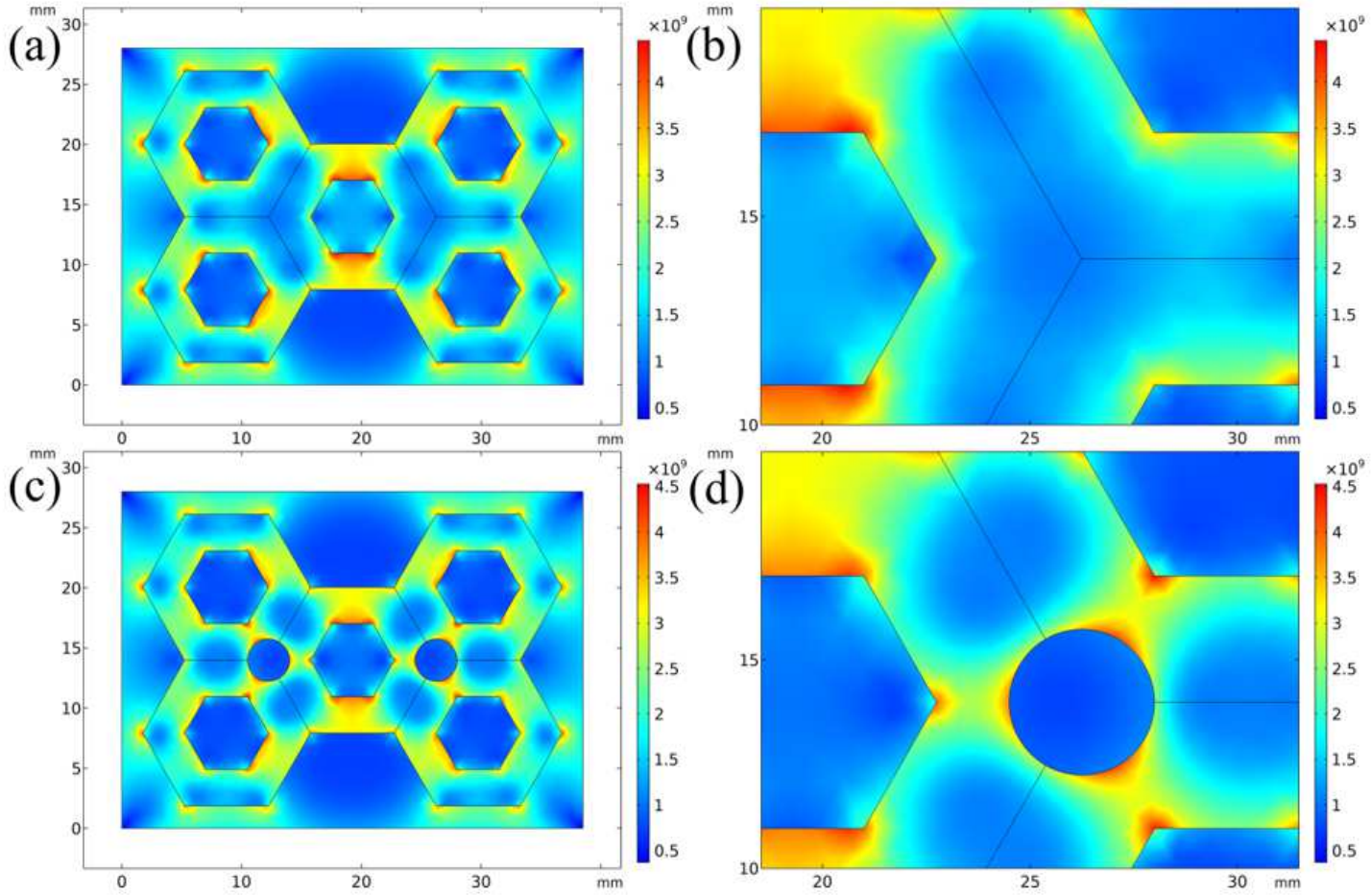

Figure 3

Thermal stress distribution during solidification in the simplified model. (a)Initial perform, (b)Partial enlarged view of the initial perform, (b)Preform with circular holes added, (d) Partial enlarged view of the perform with circular holes added.

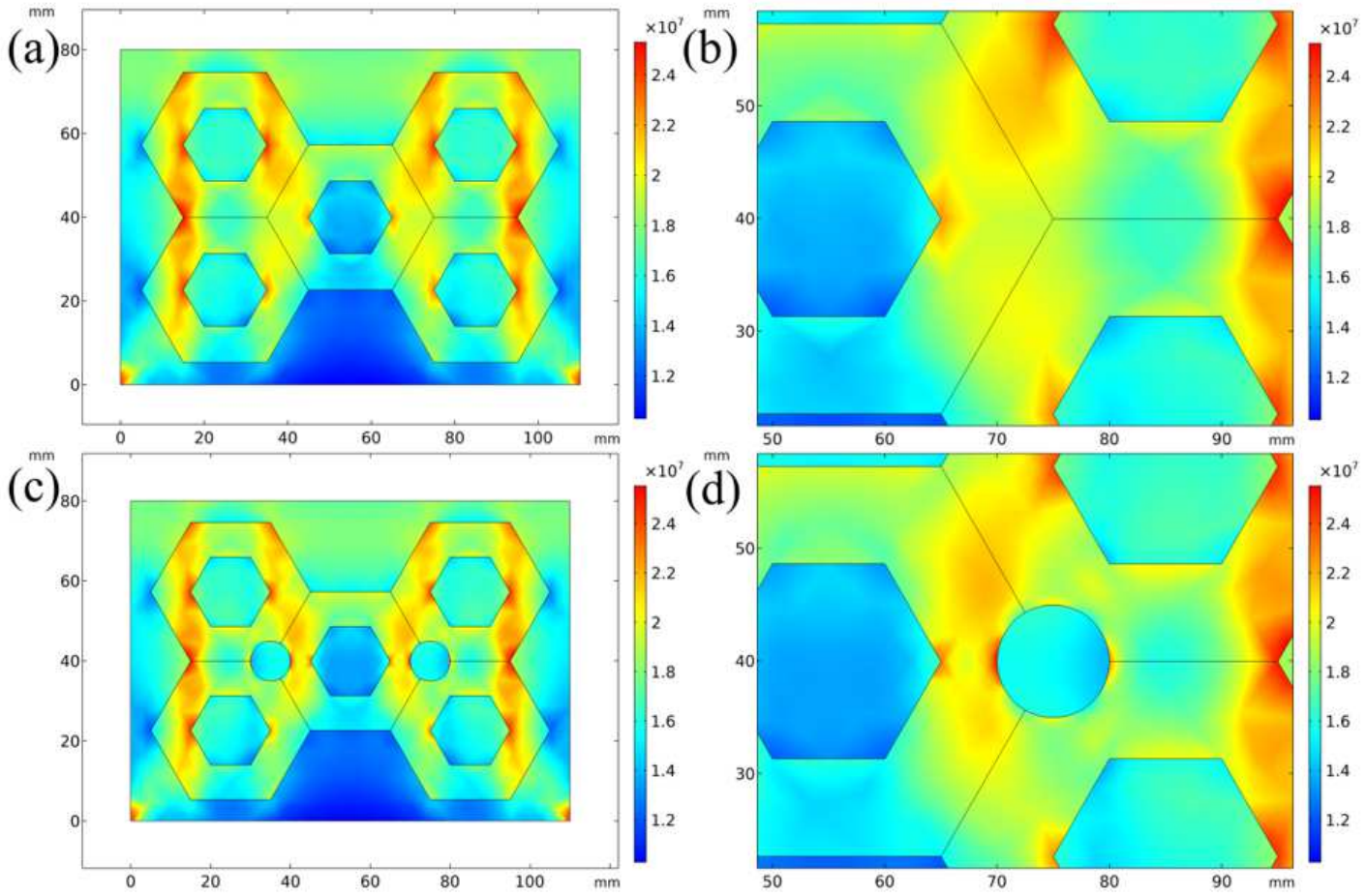

Figure 4

Compressive stress in the simplified model. (a)Initial perform, (b)Partial enlarged view of the initial perform, (b)Preform with circular holes added, (d) Partial enlarged view of the perform with circular holes added.

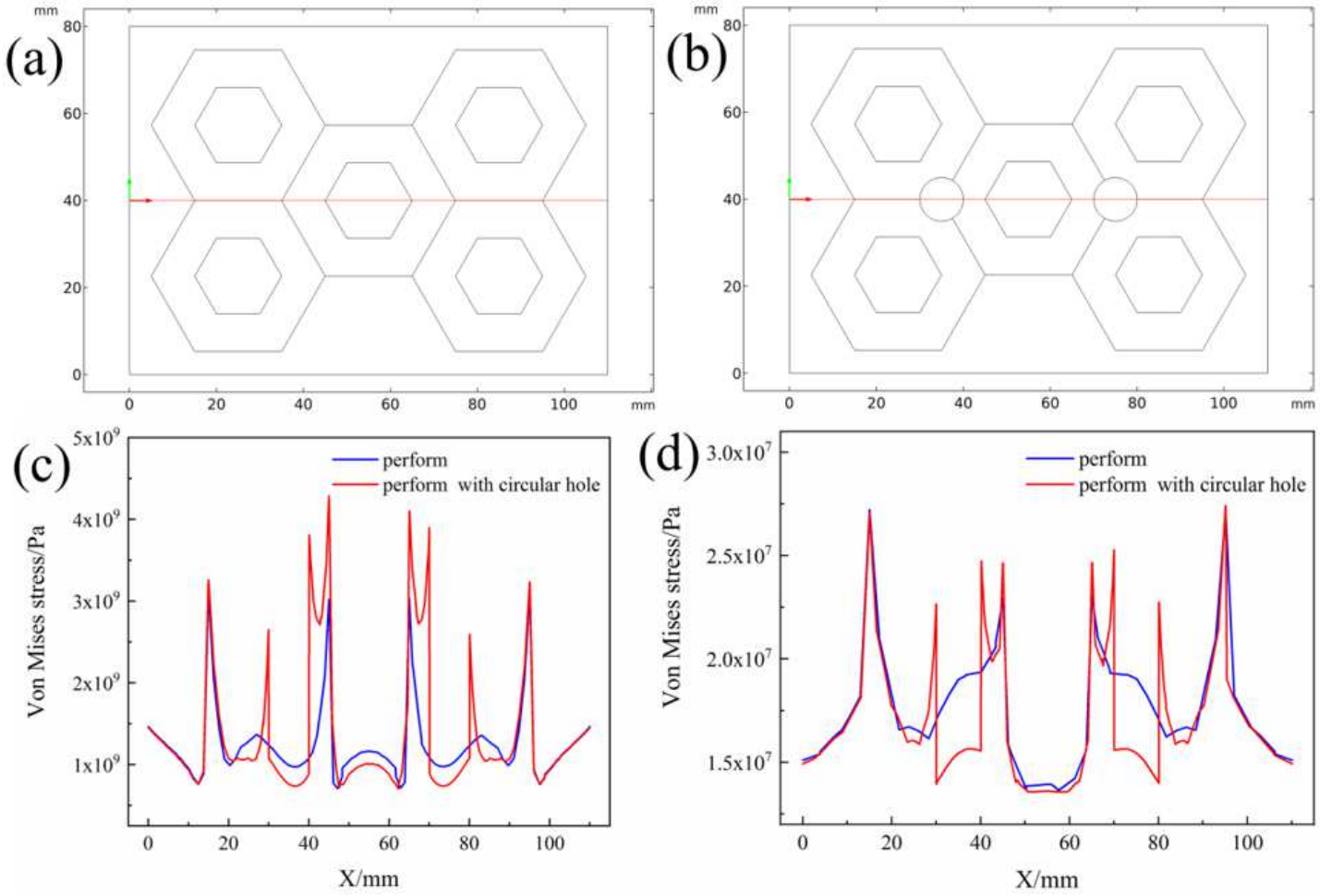

Figure 5

The position of the 2D transversal of the simplified model and stress transversal comparison, (a)Initial perform, (b)Partial enlarged view of the initial perform, (b)Preform with circular holes added, (d) Partial enlarged view of the perform with circular holes added.

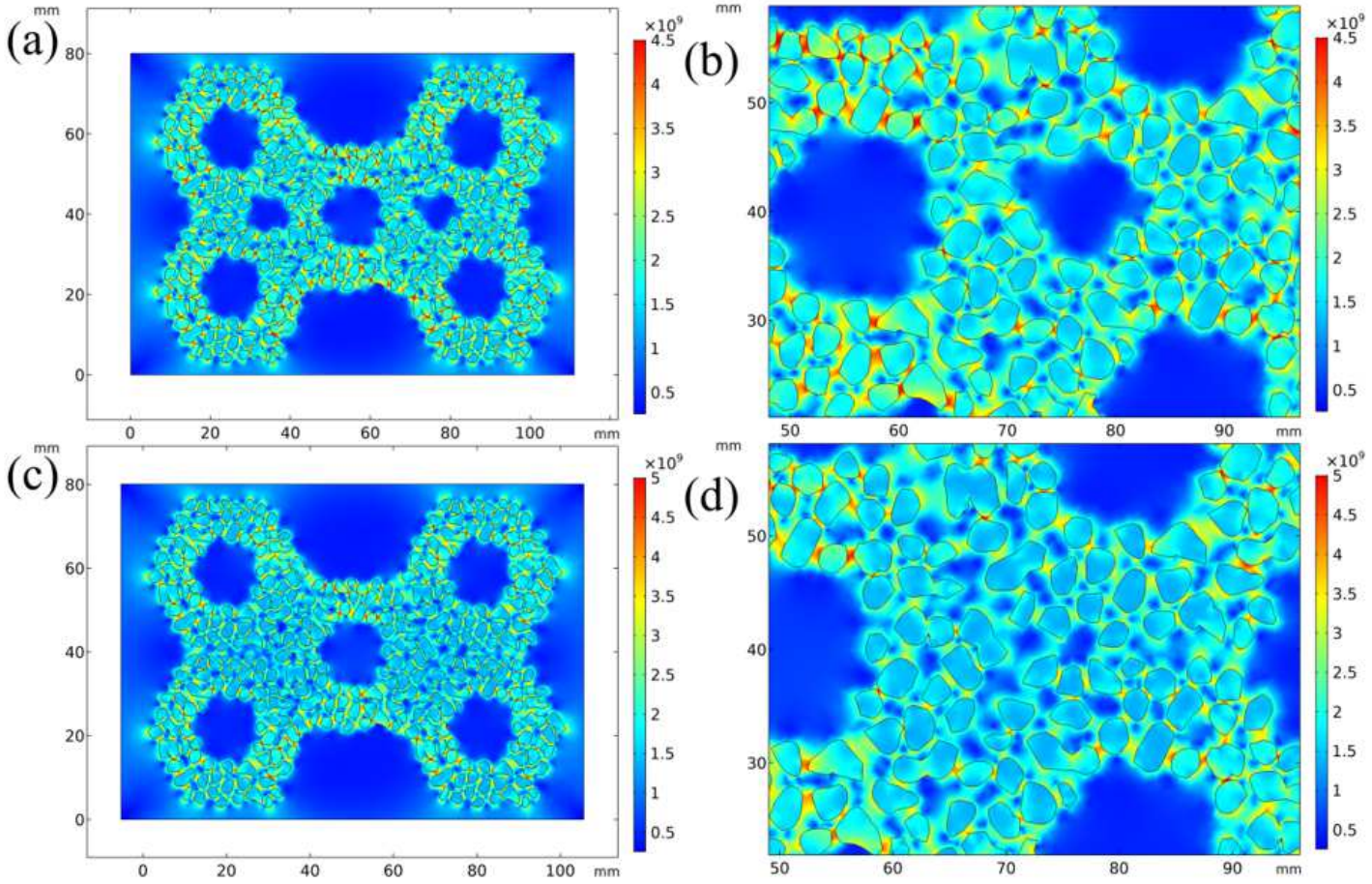

Figure 6

Thermal stress distribution during solidification in the optimized model. (a)Initial perform, (b)Partial enlarged view of the initial perform, (c)Preform with circular holes added, (d) Partial enlarged view of the perform with circular holes added.

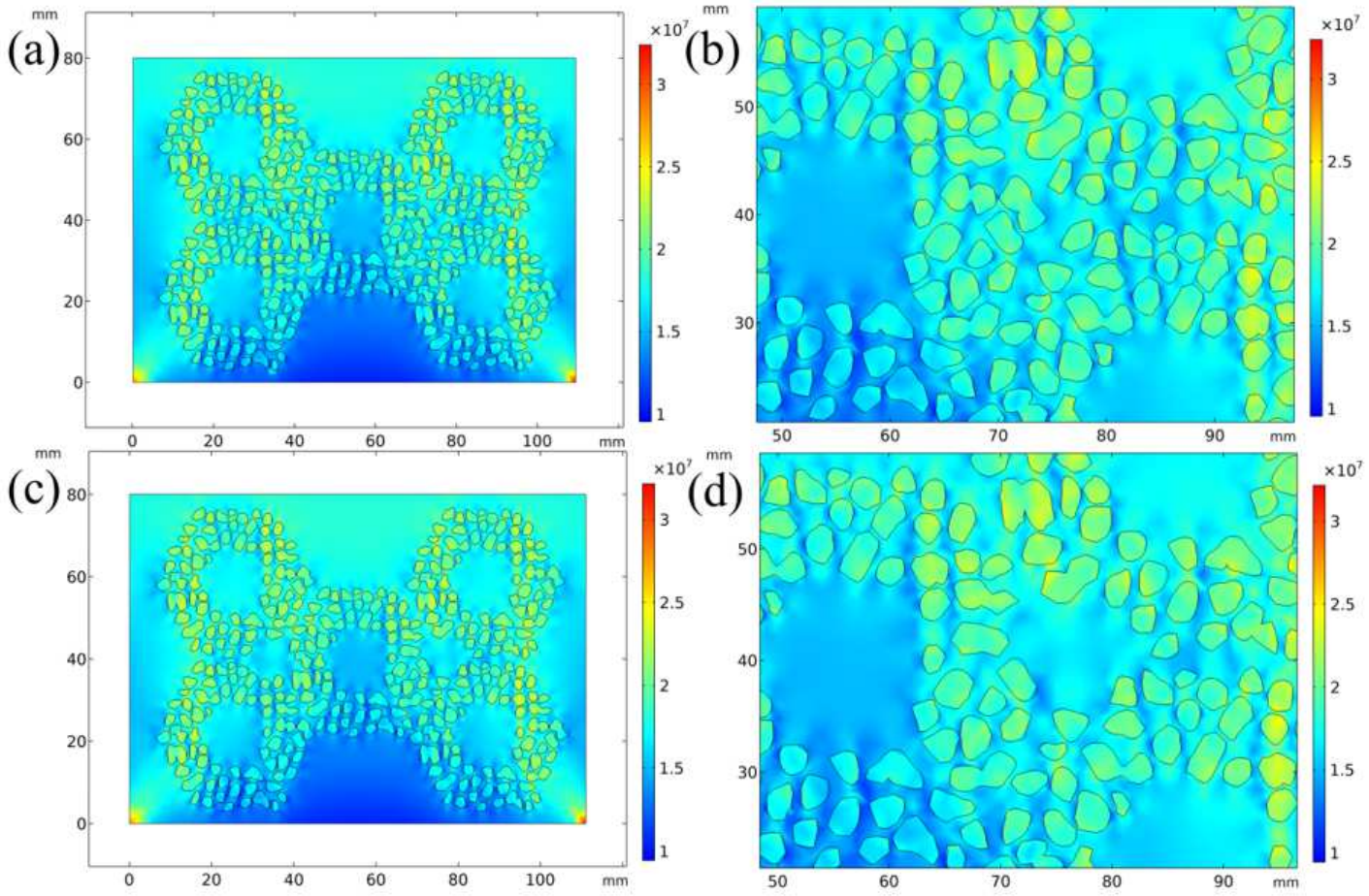

Figure 7

Compressive stress in the optimized model. (a) initial perform, (b)Partial enlarged view of the optimized perform, (c)Preform with circular holes added, (d) Partial enlarged view of the perform with circular holes added.

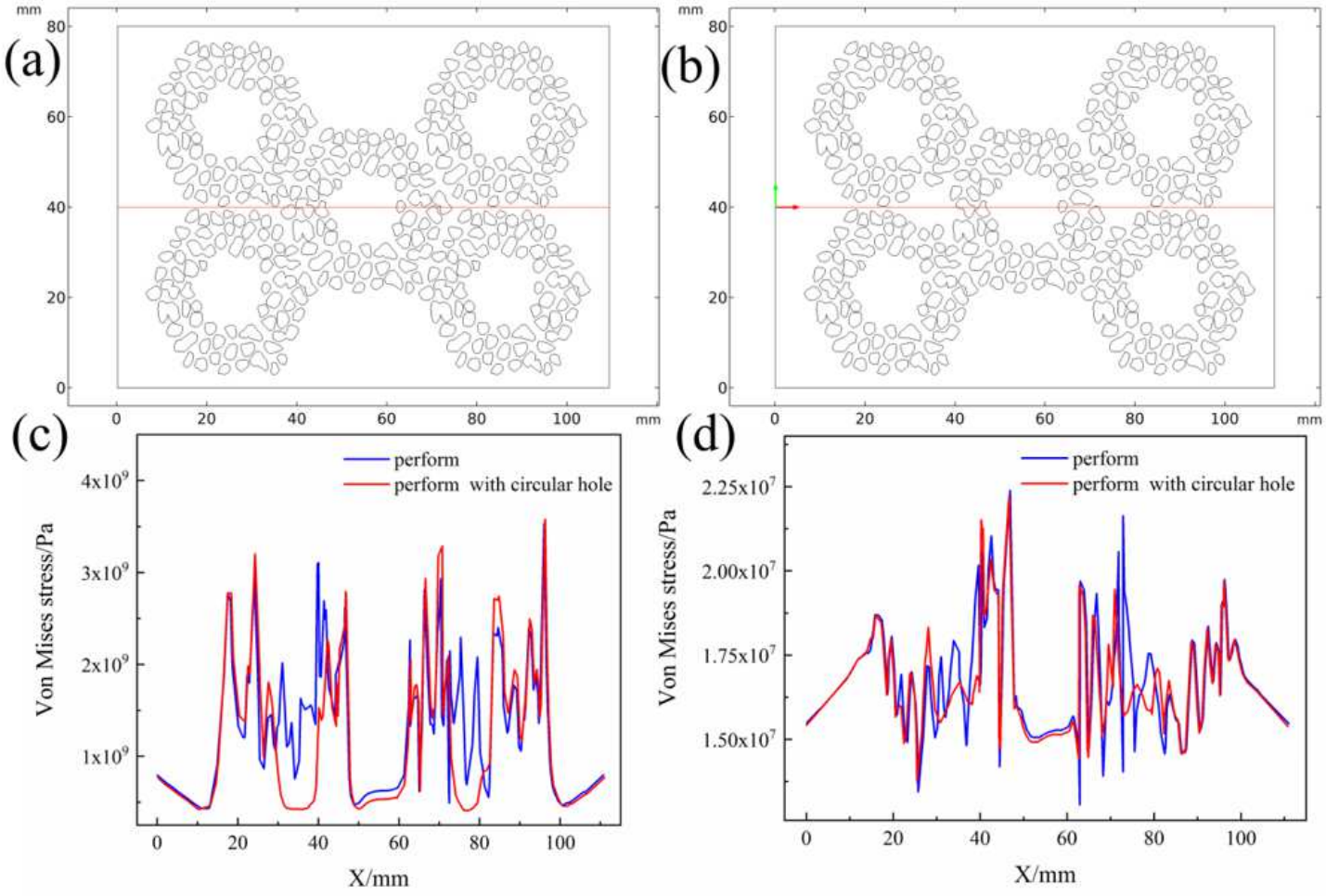

Figure 8

The position of the 2D transversal of the optimized model and stress transversal comparison. (a) Initial perform, (b) Preform with circular holes added, (c)Solidification stress, (d) compression stress.

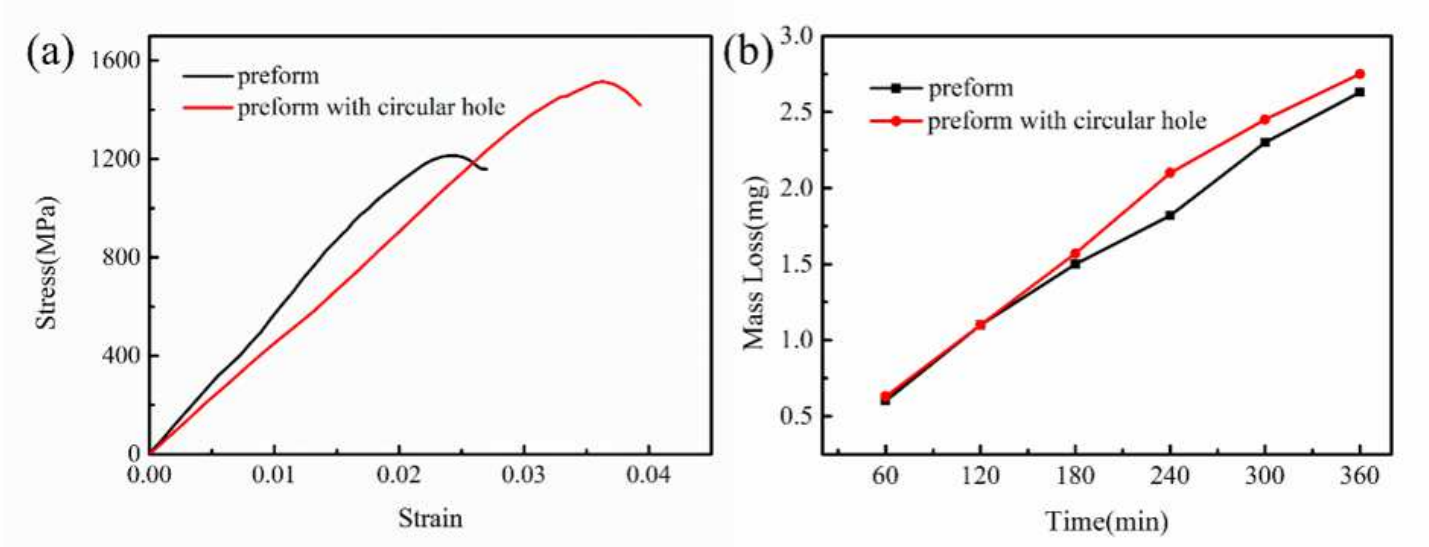

Figure 9

Compression stress-strain curve of HCCI/ZTAP composite material and mass loss of three-body abrasive at the junction of composite honeycomb walls

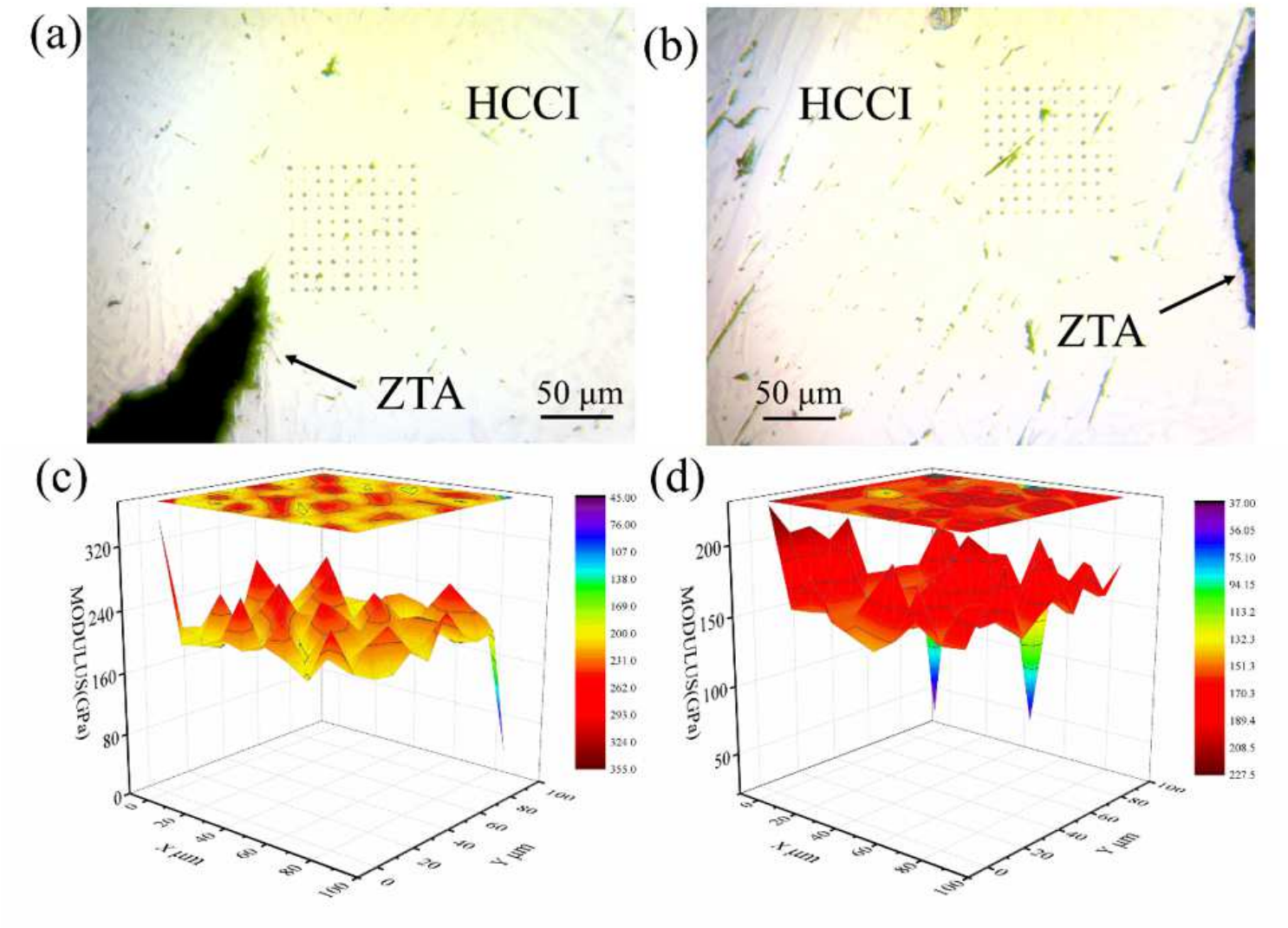

Figure 10

Indentation distribution of composite materials and the distribution of Young's modulus around the particles of composite materials.(a)The shape of the particles is sharp,(b)The shape of the particles is rounded,(c)The shape of the particles is sharp,(d)The shape of the particles is rounded.